

# Coherence of HPM generation in air

Mladen M. Kekez

**Abstract**—The effect of coherence on HPM generation has been investigated. The experimental data are presented for HPM generation in air. Coherence governs the energy content of the HPM system and demonstrates whether the system is viable or not. Coherence must be considered in the design of the resonant cavities used in high power microwave devices.

**Index Terms**— HPM generation, resonant cavity, pulse shortening, corona and spark channel discharges

## I. INTRODUCTION

THE coherence effects are not pronounced if the Heisenberg-like uncertainty principle (Ref. [1]) is used in designing the ultra-wide band system:

$$\Delta T \Delta f < 1 \quad (1)$$

$\Delta f$  is the spectral bandwidth of the source and  $\Delta T$  is the temporal duration of the pulse. The system designed by Baum *et al* [2] uses the condition specified by Eq. 1.

To facilitate the propagation of the RF/HPM over large distances, Eq. 1 explains why it is necessary to have the resonant cavity capable of producing the coherence radiation at single frequency.

In the late 19<sup>th</sup> century Nikola Tesla proposed the concept of the formation of the resonant cavity (standing waves) and the wireless transmission of energy.

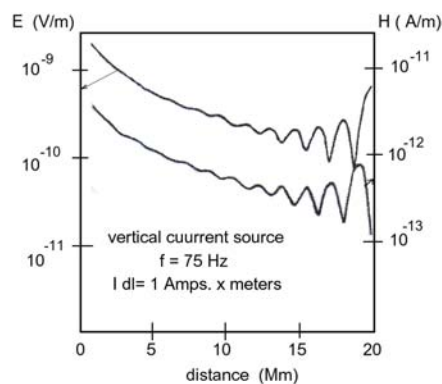


Fig. 1 shows the electromagnetic field in the earth-ionosphere waveguide by a vertical electric current course. Fig. 1 is taken from Refs. [3 and 4].

Although the rate of the radiation of energy in the form of Hertz wave, or Maxwell electromagnetic wave is very small, Tesla calculated that the electromagnetic field would start increasing at some distance from the transmitter. Tesla's calculations were confirmed in the 20 century. At the operating frequency of 75 Hz, the fields from 4 Mm (=4,000 km) show the characteristic standing wave pattern, which is most pronounced at 20 Mm. See Fig. 1.

In 1939, the Varian brothers made advancement in designing a miniature size cavity. They also added a second cavity in their experimental set-up. The device obtained was able to amplify the microwave signal. The Varian brothers called their invention: the Klystron

Over the past 50 years, efforts have been made to build better cavity suitable in handling large power: i.e., in obtaining powerful HPM sources. Benford *et al* have summarized some of these efforts in their textbook [5].

At low powers, the current theoretical description of the microwave devices appears to support well the experimental results. As the power is increased, the common problem is the early cessation of microwave production, despite the continuing propagation of the electron beam through the device.

It is suggested here that the reason for the early cessation is due to the coherence. Most HPM devices are emitting the radiation not at single frequency, but they are generating a certain bandwidth of radiation,  $\Delta f$ . In this paper limited review of HPM devices has been made and the progress noted in the design of the resonant cavity.

The concept of the coherence phenomenon is illustrated in the section II. Approximate expressions required for the analysis of data have been put forward and comparison made between the theory and the experimental evidence.

## II. COHERENCE

Coherence was initially introduced in connection with Thomas Young double-slit experiments in optics [1]. Coherence is now used in many fields that involve waves such as acoustics, electrical engineering, neuroscience and quantum mechanics.

When two waves of the same frequency are added to create a larger wave (constructive interference) or subtract from each other to create a smaller wave (destructive interference), the final result depends on their relative phase. If they have a constant relative phase, two waves are said to be coherent.

To appreciate these statements an experiment was carried out. The wave generator gave first the signal at frequency,  $f_1$  of 265 MHz. Afterwards, the signal,  $f_2$  at 275 MHz is recorded

Manuscript received December 1, 2011, revised January 31, 2012.

M. M. Kekez is with High-Energy Frequency Tesla Inc., (HEFTI), 2104 Alta Vista Drive., Ottawa, Canada, K1H 7L8, (e-mail: mkekez@magma.ca, web: [www.hefti.ca](http://www.hefti.ca))

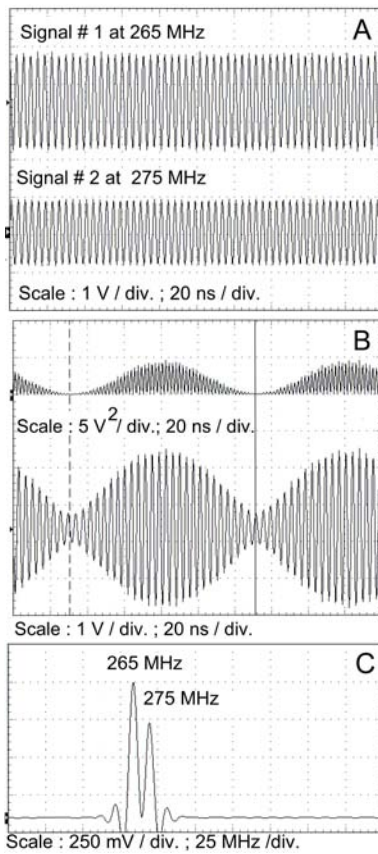


Fig. 2. Frame A shows the signals prior to the interaction. The interference of signals is given in Frame B (bottom) and the interference on power 2 is also given in Frame A (top). The FWHM ( $= \Delta f_0$ ) of 265 MHz line (or 275 MHz line) is 5.05 MHz. Combined FWHM of two signals,  $\Delta f_1$  is 17 MHz.

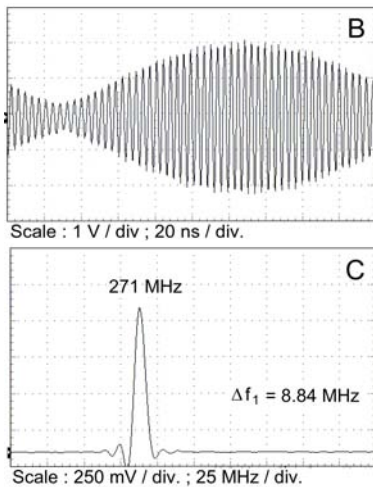


Fig. 3. Conditions are as in Fig. 2 except that the frequency of the signal #1 was changed from 265 MHz to 270 MHz

(Fig. 2, Frame A). When these signals are subtracted, the Frame B (bottom) is obtained on the oscilloscope. If the signals are added, the resulting waveform remains of the same form, except it is shifted to the left for about 50 ns. The FFT of the signal remains the same in both cases. The interference signal on power 2 is also given in Fig. 2, Frame B (top). From

Fig. 2 we see that the time interval between two adjacent peaks,  $\Delta T$  and  $\Delta f$  are related as:

$$\Delta T * \Delta f = 1 \quad \text{where } \Delta f = |f_1 - f_2| \quad (2)$$

If the full width at half magnitude (FWHM) of the signal on power two is  $\Delta t$ , Eq. 2 becomes:

$$\Delta t * \Delta f = 0.5 \quad (3)$$

In Fig. 2  $\Delta f = 10$  MHz and  $\Delta T = 100$  ns. The two vertical lines shown in Frame B are 100 ns apart and they are placed at the minimum of the interfering waveform (Frame B, bottom). If the amplitudes of signal #1 and of the signal #2 are of the same value, the interfering waveform will have zero value where the vertical lines are placed. If the amplitude of these signals is of highly different value, the small signal will perform the ‘‘amplitude modulation’’ on the large signal.

In Fig. 2,  $\Delta f_0$  is the FWHM of the single frequency. At 265 MHz (and/or 275 MHz)  $\Delta f_0$  is 5.05 MHz. Combined FWHM of two signal,  $\Delta f_1$  is 17 MHz for  $\Delta f = 10$  MHz. In Fig. 3  $\Delta f = 5$  MHz,  $\Delta f_1$  is 8.84 MHz and we have single frequency line at 271 MHz present. Now we define the parameter,  $\kappa$  as:

$$\kappa = \Delta f_1 / \Delta f \quad (4)$$

In Fig. 2  $\kappa = 17/10 = 1.7$  and in Fig. 3  $\kappa = 8.84 / 5.05 = 1.768$ . To confirm these results, measurements were made using 1.000 GHz signal and 0.990 GHz signal. The results are shown in Fig. 4. For  $\Delta f$  of 10 MHz,  $\Delta f_1$  and the parameter  $\kappa$  are of the same value as those given in Fig. 2

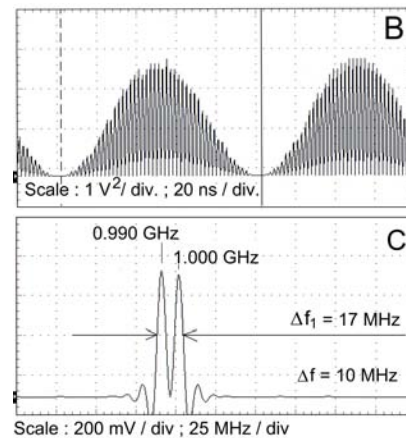


Fig. 4. Conditions are as in Fig. 2 except the interference signal is between the frequencies: of 1.000 GHz and of 0.990 GHz. These two signals are almost of the same amplitude.

From  $\Delta f_1$  we want to obtain the spectral bandwidth,  $\Delta f$  and we can get the width of the pulse,  $\Delta T$  from Eq. 2. Using  $\kappa$  to be 1.7, the experimental data are summarized in Table II.

To understand better the experimental data, an alternative approach was to do the simulation using the signal generator. Here the signal matches the width of the experimental HPM records. The signal generator produces a short pulse (see Fig. 5) at the single frequency and this frequency has the FWHM =  $\Delta f_2$  in the FFT graph.

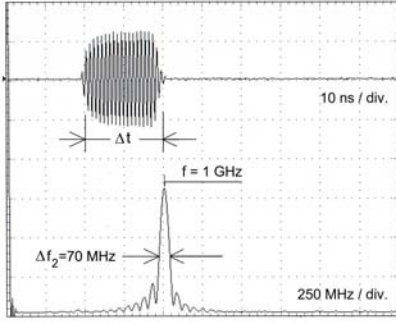


Fig. 5 shows the signal (top) and the FFT (bottom) obtained with the signal generator. To simulate experimental data we change  $\Delta t$  and frequency,  $f$

Therefore, the spectral bandwidth of the HPM source,  $\Delta f$  is

$$\Delta f \approx \Delta f_1 - \Delta f_2 \quad (5)$$

The value of  $\Delta f_2$  depends on the number of oscillations,  $N$  in the “rectangular window” used here to perform the FFT transform. If the oscillations in the pulse fill the window partially,  $\Delta f_2$  will rise as the width of the pulse is decreased. ( $\Delta f_2 \sim$  approximately  $1/N$ ). Table I is obtained with the pulse containing 1 GHz oscillations using 10 ns/div time scale.

Table I

Pulse width (ns)	20	30	40	60	70	80
$\Delta f_2$ (MHz)	70	46	34	22	18	14

### III EXPERIMENTAL CONDITIONS

The figures 6 to 10 are obtained in the set-up with the resonant cavity and the conditions described in Ref. [7]. In this arrangement the helical antenna is inserted into the resonant cavity to provide better coupling (i.e. kind of highway) between 100% reflector and partial reflector. The antenna is arranged in such ways that, RF/microwaves (radiation) wave can bounce back and forth between two mirrors in the manner analogous to the operation of laser. For a particular position of the partial reflector, for the specific value of the charging voltage applied to the Marx generator and the separation between the “hot” and “cold” electrodes, the experimental data become reproducible and self-similar. For example: after recording over 50 shots and getting the data similar to that of Figs. 6 and 7, two different shots of different kind are observed. One of them is shown in Fig. 8. Later it was observed that Fig. 8 results from the asymmetry of the spark channels distribution between hot and cold electrodes. In some cases, the asymmetry may also come from minor misalignment of the reflectors.

Fig. 9 belongs to the same family of data as Figs 6 to 8 and is obtained by the optimum separation between the hot and cold electrodes. Fig. 10 is obtained after fine-tuning of the system.

Fig. 11 is obtained during the process of tuning the cavity for the set up given in Ref [6]. In this set-up: 100% reflector, the partial reflector and the cylinder of the constant diameter provide the transport of the electromagnetic (radiation) wave. This arrangement yields significant changes in the shape of the

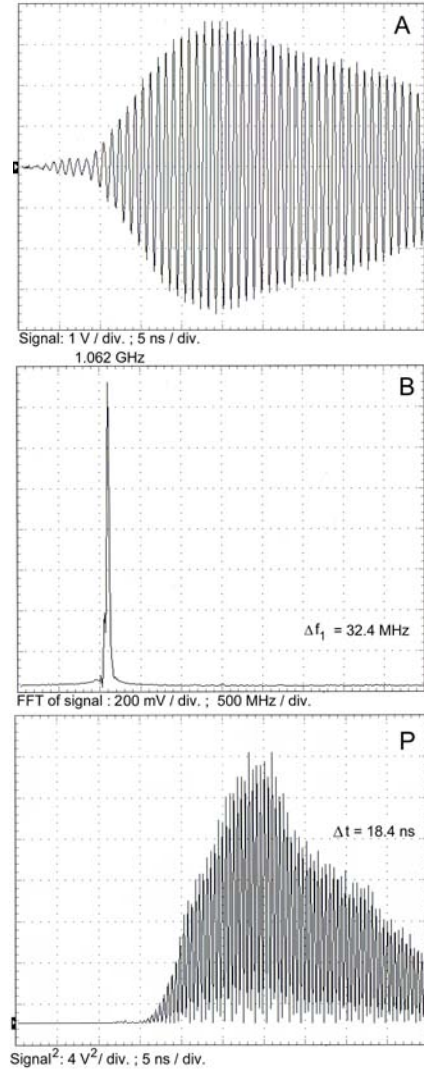


Fig. 6 Frame A is the HPM signal and Frame B is FFT of the signal. 1 GHz low pass filter was used. The energy content is  $152 \text{ V}^2\text{ns}$ . With the area of  $175 \text{ cm}^2$ , the energy content is  $0.66 \text{ J}$

pulse and its amplitude from shot to shot, because the interactions between the incident radiation wave and the reflected radiation wave from the confining side walls of the cylinder follows a rather complex path.

The waveforms were recorded with the B-dot probe and 3 GHz oscilloscope. The B-dot probe produces the signal with the amplitude that is linearly proportional (rises) with the frequency applied. Hence it is rather difficult to say whether the cavities also produce low frequency components. The amplitude of the signal of 1 Volt corresponds to the electric field of  $3.07 \text{ kV/cm}$  at frequency of 1 GHz.

### IV ANALYSIS OF THE EXPERIMENTAL DATA

It should be noted that  $\Delta f_1$  exceeds the value of the single frequency line,  $\Delta f_0$  in all the data shown in the FFT graphs. Also note that, the main frequency line radiated by the resonant cavity varies from low as 1.062 GHz to high as 1.088 GHz.

These facts show that many lines are initiated during the pre-pulse (during the charging of the cavity) and the line with

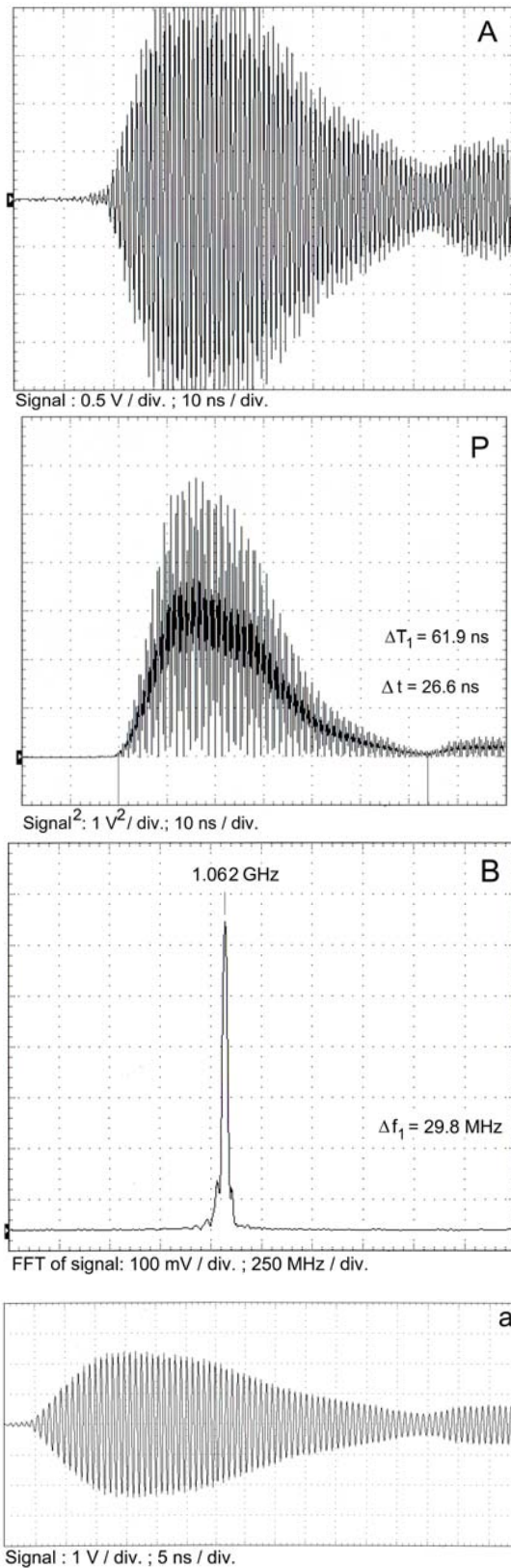


Fig. 7 Frames A and a are HPM signal and Frame B is FFT of the signal. 1.25 GHz low pass filter is used. Frame P shows the signal on power 2. The energy content is  $87 \text{ V}^2 \text{ ns}$ . With the area of  $175 \text{ cm}^2$ , the energy content is  $0.38 \text{ J}$

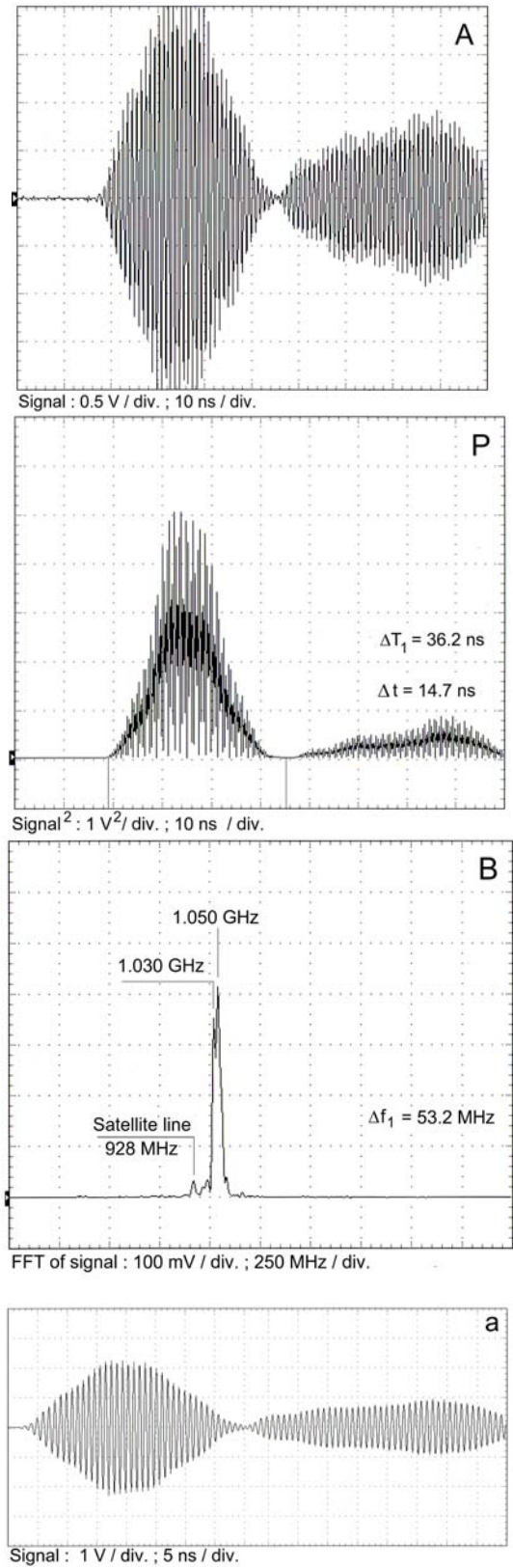


Fig. 8. Caption is as in Fig. 7. The frequency difference of  $1.050 \text{ GHz} - 0.928 \text{ GHz} = 122 \text{ MHz}$  corresponds to the period of  $8.2 \text{ ns}$ . The frequency difference of  $1.030 \text{ GHz} - 0.928 \text{ GHz} = 102 \text{ MHz}$  corresponds to the period of  $9.8 \text{ ns}$ . The energy content is  $52 \text{ V}^2 \text{ ns}$ . With the area of  $175 \text{ cm}^2$ , the energy content is  $0.23 \text{ J}$

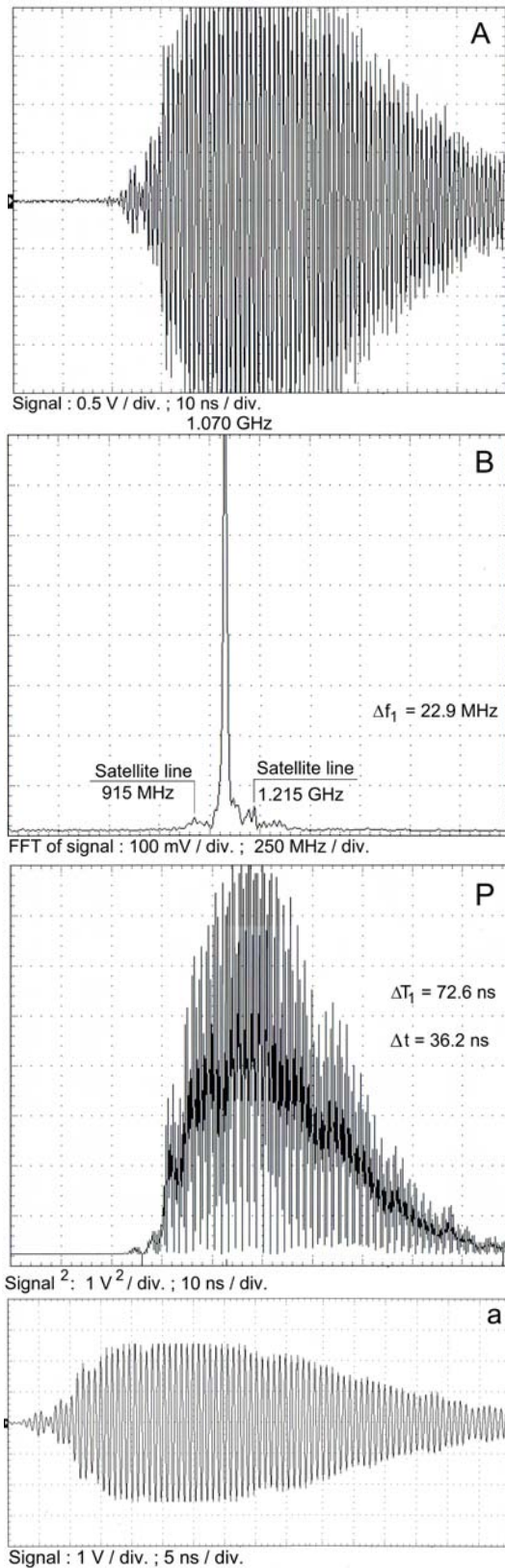


Fig. 9. Caption is as in Fig. 7. The frequency difference of 1.215 GHz- 1.070 GHz= 145 MHz corresponds to the period of 6.9 ns. The difference of 1.070- 0.915= 155 MHz corresponds to the time period of 6.45 ns. The energy content is 140 V<sup>2</sup> ns. With the area of 175 cm<sup>2</sup>, the energy content is 0.49 J

the largest intensity in  $\Delta f_1$  domain governs the final value of the frequency in the peak. This process is simulated in Fig. 3. Pertinent information given in Figs. 7 to 9 are summarized in Table II. The computation is done for  $\kappa = 1.7$ . In the experimental work the oscilloscope measures  $\Delta f_1$  and  $\Delta t$  is evaluated from the graph of the signal on power 2.

TABLE II

Figure #	$\Delta f_1$ (MHz)	$\Delta f = \Delta f_1 / \kappa$ (MHz)	$\Delta t$ (ns)	$\Delta f * \Delta t$	$\Delta T$ (ns)
7	29.8	17.53	26.6	0.466	57
8	53.2	31.3	14.7	0.460	32
9	22.9	13.47	36.2	0.488	74

It should be noted that in Table II the product of  $\Delta f$  times  $\Delta t$  supports Eq. 3. Also, the computed value for  $\Delta T$  is obtained from Eq. 2 ( $\Delta T = 1 / \Delta f$ ) is in close agreement with the width of the (first) pulse,  $\Delta T_1$  (defined as the distance between the vertical lines) shown in Frame P for Figs. 7 to 9.

Table III is obtained using Eq. 5. The experimental data for Table III are recorded with 10 ns/div. time scale and with the FFT scale of 250 MHz/div. This makes possible to get the value for  $\Delta f_2$  from Table I. In Table III the product of  $\Delta f$  times  $\Delta t$  differs from Eq. 3.

Table III

Figure #	$\Delta f_1$ (MHz)	$\Delta f_2$ (MHz)	$\Delta f$ (MHz)	$\Delta t$ (ns)	$\Delta f * \Delta t$
7	29.8	14	15.8	26.6	0.420
8	53.2	14	39.2	14.7	0.576
9	22.9	14	8.9	36.2	0.322

Figs. 8 to 9 show the presence of the satellite lines that are observed well in Fig. 10. The frequency difference of these lines in respect to the main line in the FFT plot gives the time period of the signals. These satellite lines are performing the “amplitude modulation” on the (main) HPM line.

If the data shown in Fig. 10 are recorded with 20 ns/div. time scale, the coherence effect is not noticeable for the period of 200 ns. It was also observed that only Marx generator governs the overall characteristics of HPM emissions. Fig. 11 offers direct support to the concept proposed by Eq. 2.

#### IV CONCLUSIONS

The concept that the satellite lines have to be of smaller amplitude in respect to the main (carrier) frequency, is used in AM and FM radio.

When the interaction between the signals of different frequency takes place, the law of the conservation of energy holds. Cancellation of any (particular) line is “virtual” because the wave cannot have negative energy. The “valleys” between the burst of the pulses shown in Fig. 11 signifies that the energy from the frequencies around 2 GHz is being transferred only to the energy of low frequency components that B dot

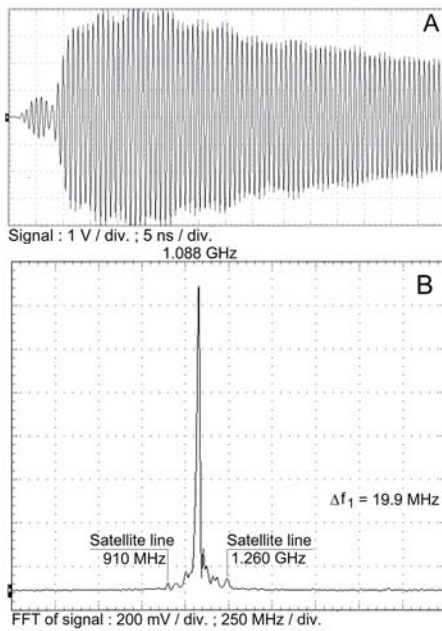


Fig. 10. Caption is as in Fig. 7. The difference of 1.260 GHz-1.088 GHz= 172 MHz corresponds to the period of 5.8 ns. The difference of 1.088-0.910= 178 MHz corresponds to the time period of 5.6 ns. The energy content is  $375 \text{ V}^2\text{ns}$ . With the area of  $175 \text{ cm}^2$ , the energy content is 2.14 J.

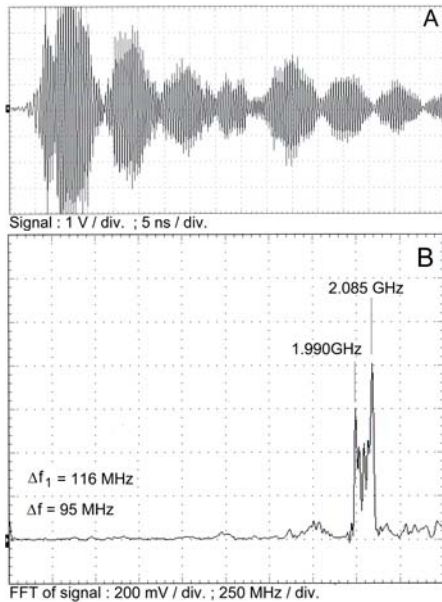


Fig. 11. Caption is as in Fig. 7 except that the filter is not used. The frequency difference of 2.085-1.990= 95 MHz corresponds to the period of 10.5 ns. The distance between the maximum of burst of the pulses shown in the frame A is in the range of 10 to 11 ns.

probe cannot detect well. If the source is producing the coherent radiation, the product of the distance measured from the cavity to some point in space,  $d$  times the electric field,  $E$  at this point, must be constant (i.e.,  $E \cdot d = \text{constant}$ ). When this does not occur the electric field falls rapidly if the distance is increased slightly. Coherence can be understood when the ultra-wide band system is producing the pulse of longer duration. Such system does not obey Eq. 1 and the coherence phenomenon is pronounced well. See Ref. [8].

The question remains whether Eq. 3 can account for the microwave pulse width limit (pulse shortening) observed by most scientists working on the BWO. Shifts in frequency (or “chirping”) have been observed in most BWO and Vircators.

By improving the resonant cavity Tot'meninov *et al* [9] have made the BWO to radiate at 3.65 GHz with a pulse width,  $\Delta t$  of 16 ns and the maximum power of  $3.4 \pm 0.7 \text{ GW}$ . In this system  $\Delta f_1$  is about 100 MHz (Prof. V.V. Rostov; private communication). I find  $\Delta f_2$  to be 70 MHz for 20 ns pulse at 3 GHz. Tentatively,  $\Delta f = \Delta f_1 - \Delta f_2 = 100 \text{ MHz} - 70 \text{ MHz} = 30 \text{ MHz}$ . This makes  $\Delta t * \Delta f$  to be 0.48. This is in accord with Eq. 3.

Prasad *et al* [10] gave data on 4 GHz, 600 MW magnetron. I find that their system has  $\Delta t = 5.85 \text{ ns}$  and  $\Delta f_1 = 178 \text{ MHz}$ . Detailed value of  $\Delta f_2$  is required before we can see whether their data supports Eq. 3. If their resonators in the magnetron would be of elliptical shape instead of the current circular shape, it would be possible to decrease  $\Delta f$  and increase  $\Delta t$ .

To achieve the next generation of HPM devices with higher power and larger energy content, we require full understanding of interaction of the electromagnetic (radiation) waves with the electron beams and plasma in the resonant cavity. Also, we need to design the resonant cavity that will have zero  $\Delta f$ , no “chirping” and no satellite lines.

We may now start to appreciate the ideas of Nikola Tesla and the data given in Fig. 1. Tesla used 75 Hz signal because the low frequency has low attenuation as a function of distance, and because  $\Delta f$  is made small at low frequencies. Tesla gave us an approach to have a good earth-ionosphere waveguide / resonator.

## REFERENCES

- [1] <http://en.wikipedia.org/wiki/Coherence>
- [2] C. E. Baum, W.L. Baker, W. D. Prather, J. M. Lehr, L. P. O'Loughlin, D. V. Giri, I. D. Smith, R. Altes, J. Fockler, D. McLemore, M. D. Abdalla and C. Skipper, JOLT: A highly directed, very intensive impulse like radar, *Proceedings of IEEE*, 2004, **92**, p 1096.
- [3] A. S. Marinčić, Nikola Tesla and wireless transmission of energy, *IEEE Trans. on Power Apparatus and Systems*, 1982, **PAS- 101**, pp 4064-4067
- [4] M. L. Burrows, *ELF communication antennas*, Stevenage Peter Peregrinus, 1978
- [5] J. Benford, J. A. Swegle and E. Schamiloglu, *High Power Microwaves*, Second editions, (NY; Taylor & Francis Group), 2007
- [6] M. M. Kekez, Description of HPM generation in atmospheric air using the laser and klystron terminology, 2011 (published on web: <http://www.hefti.ca/>)
- [7] M. M. Kekez, Details of HPM generation in atmospheric air using the laser and klystron terminology, 2011 (published on web: <http://www.hefti.ca/>)
- [8] M. M. Kekez, HPM generation in atmospheric air, *Proc. the 13 Int. Conf. on Megagauss magnetic field generation and related topics, Suzhou, China*, 2010 (also published on web: <http://www.hefti.ca/>)
- [9] E.M. Tot'meninov, P.V. Vykhodsev, S. A. Kitsanov, A. I. Llimov and V. V. Rostov, Relativistic backward-wave tube with mechanically tunable generation frequency over 14% range, *Technical Physics*, **56**, pp 1009-1012, 2011
- [10] S. Prasad, M Roybal, C. J. Buchenauer, K. Prestwich, M. Fuks, and E. Schamiloglu, Experimental verification of the advantages of the transparent cathode in a short-pulse Magnetron, *Proc. 17th IEEE Conf. on Pulsed Power, Washington., USA*, June 2009, pp. 81-85

BIOGRAPHY: (NOT AVAILABLE)

## APPENDIX

The appendix offers additional support for Eq. 2 and Eq. 5.

Fig. 1 given below gives an additional support for Eq. 2. Here,  $\Delta T$  (=distance between the vertical lines) is 63 ns and with  $\Delta f=13$  MHz, the product of  $\Delta f$  times  $\Delta T$  becomes 0.819. Eq. 2 states that  $\Delta f$  times  $\Delta T=1$ . Hence, the experimental data differs from Eq. 2 by 18.1 %.

Eq. 5 states that:  $\Delta f \approx \Delta f_1 - \Delta f_2$ . Here  $\Delta f_2$  is the FWHM of the signal produced by the signal generator. Eq. 5 is accurate if the pulses for both  $\Delta f_1$  and  $\Delta f_2$  are of the same shape.

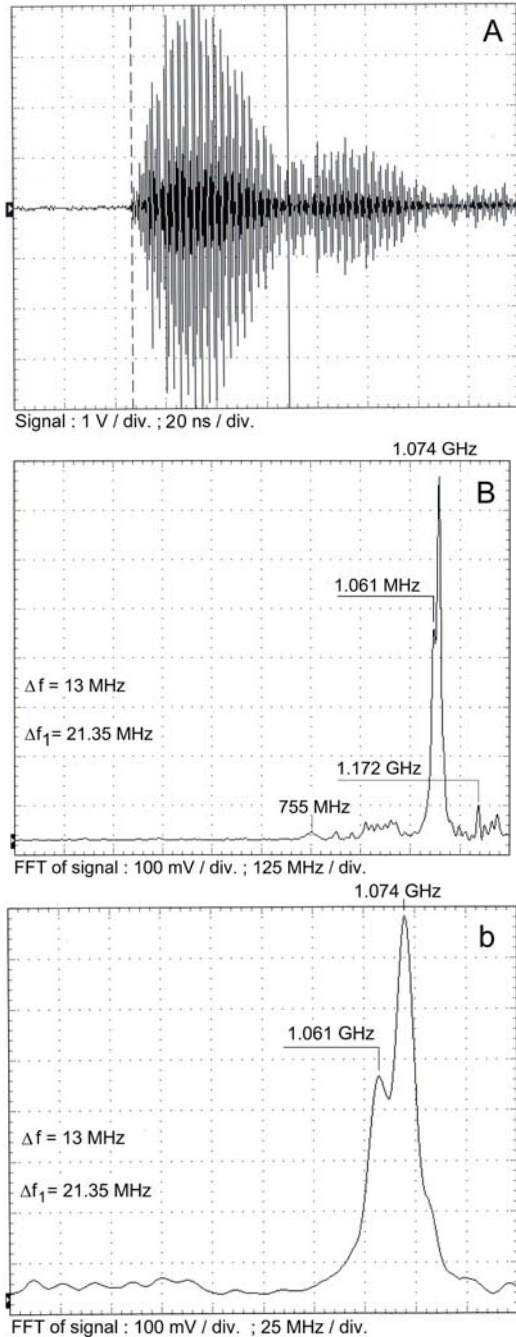


Fig. 1 is obtained during the tuning of the resonant cavity to obtain Fig. 10. Frames B and b are the FTT of the signal.

Fig. 2 given below is one examples of many data recorded when the cavity is tuned well and where Eq. 5 can be applied with confidence.

For the experimental data shown in Fig 2, the signal generator gives that  $\Delta f_2$  is 8.56 MHz.

Putting the values  $\Delta f_1$  and  $\Delta f_2$  into Eq. 5 it can be stated that the coherence effects are not evident.

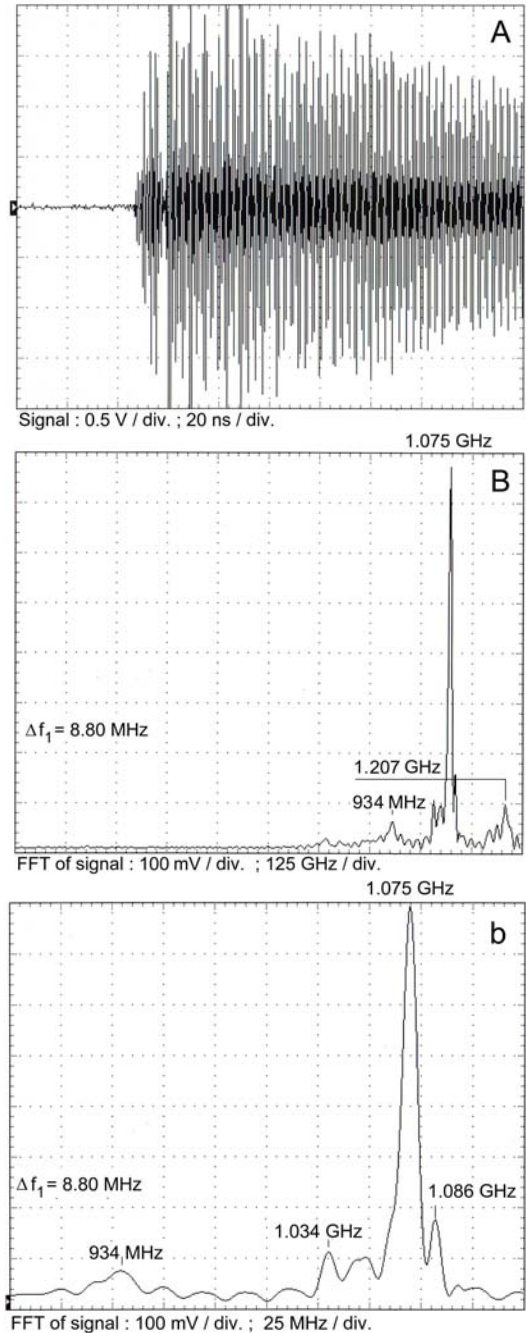


Fig. 2. The experimental conditions are similar to that of Fig. 10. Frames B and b are the FTT of the signal.